

Quantifying the Information Leak in Cache Attacks through Symbolic Execution

Sudipta Chattopadhyay
Saarland University

Moritz Beck
Saarland University

Ahmed Rezine
Linköping University

Andreas Zeller
Saarland University

Abstract—Cache timing attacks allow attackers to infer the properties of a secret execution by observing cache hits and misses. But how much information can actually leak through such attacks? For a given program, a cache model, and an input, our CHALICE framework leverages symbolic execution to compute the amount of information that can possibly leak through cache attacks. At the core of CHALICE is a novel approach to quantify information leak that can highlight critical cache side-channel leaks on arbitrary binary code. In our evaluation on real-world programs from OpenSSL and Linux GDK libraries, CHALICE effectively quantifies information leaks: For an AES-128 implementation on Linux, for instance, CHALICE finds that a cache attack can leak as much as 127 out of 128 bits of the encryption key.

1. Introduction

Cache timing attacks [11] are among the best known *side channel* attacks to determine secret features of a program execution without knowing its input or output. The general idea of a timing attack is to observe, for a known program, a timing of cache hits and misses, and then to use this timing to determine or constrain features of the program execution, including secret data that is being processed.

The precise nature of the information that *can* leak through such attacks depends on the cache and its features, as well as the program and its features. Consequently, given a model of the cache and a program run, it is possible to analyze which and how much information would leak through a cache attack. This is what we do in this paper. Given a program execution and a cache model, our CHALICE approach automatically determines *which bits of the input would actually leak through a potential cache attack*.

As an example, consider an implementation of the popular AES encryption algorithm. Given an input and an encryption key (say, 128 bits for AES-128), CHALICE can determine which and how many of the bits of the key would leak if the execution were subject to a cache attack. To this end, CHALICE uses a novel *symbolic execution* over the given concrete input. During symbolic execution, CHALICE derives symbolic timings of cache hits and misses; these then again reveal under which circumstances individual bits of encryption key may leak.

The reason why CHALICE works is that the timings of cache hits and misses are not uniformly distributed; and therefore, some specific timings may reveal more information than others. Figure 1 demonstrates the execution of an

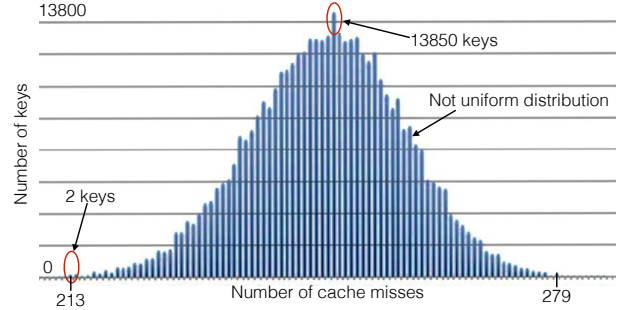


Figure 1. For a fixed input message, the plot shows the number of keys leading to a given number of cache misses incurred by executing AES-128 encryption (sample size = 256000 keys)

AES-128 implementation [1] for a fixed input and 256,000 different keys, inducing between 213 and 279 cache misses. We see that the distribution of cache misses is essentially Gaussian; if the number of cache misses is average, there are up to 13,850 keys which induce this very cache timing. If we have an extreme cache timing with 213 misses (the minimum) or 279 misses (the maximum), then there are only 2 keys that induce this very timing. CHALICE can determine that for these keys, 90 of 128 bits would leak if the execution were subjected to a cache attack, which in practice would mean that the remaining 38 bits could be guessed through brute force—whereas other “average” keys would be much more robust. For each key and input, CHALICE *can precisely predict which bits would leak*, allowing its users to determine and find the best alternative.¹

It is this *precision of its symbolic analysis* that sets CHALICE apart from the state of the art. Existing works [16] [21] use static analysis alone to provide an upper bound on the potential number of different observations that an attacker can make. This upper bound, however, does not suffice to choose between alternatives, as it ignores the *distribution of inputs*: It is possible that certain inputs may leak substantially more information than others. Not only that such an upper bound might be imprecise, it is also incapable to identify inputs that exhibits substantial information leakage through side channels. Given a set of inputs (typically as part of a testing pipeline), CHALICE

1. In the best of all worlds, one might have an implementation of every critical algorithm, such as an encryption routine, to have a uniform distribution over cache misses. But neither does such implementations exist that would be efficient, nor do we know whether such implementations *can* exist; and replacing a well-studied algorithm like AES by some other algorithm with uniform distribution may induce other, yet unknown risks.

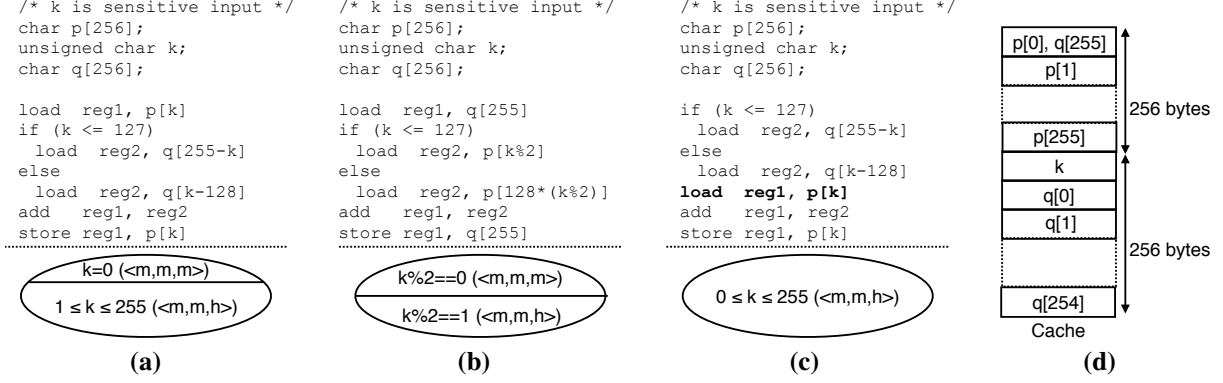


Figure 2. k is a sensitive input. (a)-(c) three code fragments and respective partitions of the input space with respect to cache hit/miss sequence ($reg1$, $reg2$ represent registers), (d) mapping of program variables into a direct-mapped cache sized 512 bytes ($q[255]$ and $p[0]$ conflict in the cache)

can precisely quantify the leak for each input, and thus provide a full spectrum that characterizes inputs with respect to information leakage.

The remainder of this paper is organized as follows. After giving an overview on CHALICE (section 2), we make the following contributions:

- 1) We present CHALICE, *a new approach to precisely quantify information leak in execution* and its usage in software testing (section 3).
- 2) We introduce *a symbolic cache model* to instantiate CHALICE to detect cache side channel leakage (section 4). This is the first usage of symbolic execution to explore cache states along with the program states.
- 3) We demonstrate that the model generalizes across *multiple observer models*. section 5 demonstrates how CHALICE is instantiated for both direct-mapped and LRU cache replacement policies.
- 4) We provide an *implementation* (section 6) based on LLVM and the KLEE symbolic virtual machine. Source code of CHALICE and all experimental data will be publicly available in the following URL:
<https://bitbucket.org/sudiptac/cache-side-channel>
- 5) We *evaluate* our CHALICE approach (section 7) to show how we quantify the information leaked through execution in several libraries, including OpenSSL and Linux GDK libraries, and show that the information leak can be as high as 251^{16} for certain implementations [1] of AES-128.

After discussing related work (section 8), we close with conclusion and consequences (section 9).

2. Overview

In this section, we convey the key insight behind our approach through examples. In particular, we illustrate how CHALICE is used to quantify information leak from the execution trace of a program.

Motivating Example

Let us assume that our system contains a direct-mapped cache of size 512 bytes. Figures 2(a)-(c) show different code fragments executed in the system. For the sake of clarity, we use both assembly-level and source-level syntaxes. However, our framework takes a binary code as input, in order to accurately capture the memory behaviour of a program. For simplicity in the example, we assume that conditional checks do not involve any access to cache (*i.e.* k is assigned to a register). The mapping of different variables into the cache is shown in Figure 2(d). Let us assume that the code fragments of Figures 2(a)-(c) are executed with some arbitrary (and unknown) value of k . Broadly, CHALICE answers the following question: *Provided only the cache performance (e.g. cache hit/miss sequence) from such executions, how much information about the sensitive input k is leaked?*

The cache performance induces a partition on the program input space. Let us capture the cache performance via a sequence of hits (h) and misses (m). In Figure 2(a), for all values of k between 0 and 127, we observe two cache misses due to the first two memory accesses, $p[k]$ and $q[255 - k]$, respectively. The second access to $p[k]$ is a *cache hit*, for $k \in [1, 127]$. However, if $k = 0$, the content of $p[k]$ will be replaced by $q[255 - k]$, resulting in a cache miss at the second access of $p[k]$. For $k \in [128, 255]$, $p[k]$ is never replaced once it is loaded into the cache. Therefore, the second access to $p[k]$ is a cache hit for $k \in [128, 255]$. In other words, we observe the sequence of cache hits and misses to induce the following partition on the input space: $k = 0$ (hit/miss sequence = $\langle m, m, m \rangle$) and $k \in [1, 255]$ (hit/miss sequence = $\langle m, m, h \rangle$). A similar exercise for the code in Figure 2(b) results in the following partition of the sensitive input space: $k \in [0, 255] \wedge k \bmod 2 = 0$ (hit/miss sequence = $\langle m, m, m \rangle$) and $k \in [0, 255] \wedge k \bmod 2 \neq 0$ (hit/miss sequence = $\langle m, m, h \rangle$).

Key observation. In this work, we stress the importance of *quantifying information leaks from execution traces and not from the static representation of a program*. To illustrate this, consider the input partitions created for code fragments

in Figures 2(a)-(b). We emphasize that observing the cache hit/miss sequence $\langle m, m, m \rangle$, from an execution of the code fragment in Figure 2(a), results in complete disclosure of sensitive input k . On the contrary, observing the sequence $\langle m, m, m \rangle$, from an execution of the code fragment in Figure 2(b), will only reveal the information that k is odd. Such information still demands a probability of $\frac{1}{128}$ in order to correctly guess k at first attempt. This is in contrast to accurately guessing the correct value of k at first attempt (as happened through the sequence $\langle m, m, m \rangle$ for Figure 2(a)). In order to fix the cache side-channel leak in Figure 2(a), we can reorder the code as shown in Figure 2(c).

Limitations of static analysis. Existing works in static analysis and verification have aimed at quantifying side channel leaks [16], [21] and verifying constant-time implementations [7], [10]. These works correlate the number of possible observations (by an attacker) with the number of bits leaked through a side channel. We believe this view can be dangerous. Indeed, both code fragments in Figures 2(a)-(b) have exactly two possible cache hit/miss sequences, for arbitrary values of k . Therefore, approaches based on static analysis [16], [21] will consider these two code fragments *equivalent* in terms of cache side-channel leakage. As a result, statically analyzing a program will not reveal crucial information leak scenarios, such as the execution of code fragment in Figure 2(a) with $k = 0$. Techniques based on verifying that programs execute in constant time typically check that memory accesses do not depend on sensitive inputs. Yet, most implementations do not execute in constant time. Besides, programs such as in Figure 2(c) have accesses that may depend on sensitive inputs without leaking information about it to a cache-performance observer. Therefore, we not only check the dependency between accessed memory address and program inputs, but we also accurately track the information flow through cache performance.

Can we use dynamic tainting? In the preceding paragraph, we state the importance of dynamically tracking sensitive information flow through cache performance. Approaches based on dynamic taints [13] can accomplish the task to detect information leak through standard functional outputs. However, such approaches fail to detect information leak through software non-functional outputs, such as cache performance, among others. Our methodology targets this angle of information leak detection by building a relationship between sensitive inputs and observed cache performance. In order to establish such a relationship, we leverage on symbolic analysis and constraint solving.

Limitations of side-channel vulnerability metrics. In contrast to existing works on measuring cache side channel leakage [15], we do not aim to check the strength of an attacker to *observe information through side channel*. Although promising, this work [15] *fails* to detect the information flow between sensitive inputs and observed performance. As a result, the side-channel vulnerability metric can only quantify *how well* an attacker can retrieve information

from a system, but, *does not highlight the information potentially leaked to the attacker*. Of course, we believe our work is complementary to the metrics proposed in [15] and CHALICE could be combined with such metrics to build more advanced metrics for measuring side channel leakage. Such metrics could consider both information leaked by the system as well as the information that could be retrieved by an attacker.

The usage of CHALICE. CHALICE is aimed to be used for validating security properties of software. Given a test suite (*i.e.* a set of concrete test inputs) for the software, CHALICE is used to quantify the information leaked for each possible observation obtained from this test suite. This is possible, as the observation by an attacker (*e.g.* number of cache miss) corresponds to a (set of) test inputs and CHALICE presents how much can be deduced about such inputs from the respective observation. In other words, our framework CHALICE fits the role of a *test oracle* [9] in the software validation process. For instance, if CHALICE reports substantial information leakage, the test inputs leading to the respective observation should be avoided (*e.g.* avoiding a “weak” encryption key) or the candidate program needs to be restructured to avoid such information leak. The generation of an effective and optimized test suite, in order to detect cache side channels, is an open problem. However, CHALICE can be instantiated to generate a witness for each possible observations made by an attacker. The set of all these witnesses forms a concise test suite and our proposed method in CHALICE can quantify information leak for each element in such a test suite. In this paper, we only focus on the quantification of information leak in a single test execution and not on the generation of a test suite.

CHALICE *should not* be used for verifying the absence of cache side-channel leakage. Implementations that must adhere to zero-leakage, may leverage on CHALICE during the early design, specifically to discover the severity of potential cache side-channel leaks and the program locations exhibiting such leaks. Nevertheless, CHALICE is aimed for testing arbitrary software and we envision that such a strategy becomes an integral component of software testing pipeline in the future.

How CHALICE works. Let us assume that we execute the code in Figure 2(a) with some input $I \in [0, 255]$ and observed the trace $t_I \equiv \langle m, m, m \rangle$. *Given only the observation t_I , CHALICE quantifies how much information about program input I is leaked.* CHALICE symbolically executes the program and it tracks all memory accesses dependent on the sensitive input k . For each explored path, CHALICE constructs a symbolic cache model, which accurately encodes all possible cache hit/miss sequences for the respective path. In this example, CHALICE constructs $\Gamma(0 \leq k \leq 127)$ and $\Gamma(128 \leq k \leq 255)$, which encode all cache hit/miss sequences for inputs satisfying $0 \leq k \leq 127$ and $128 \leq k \leq 255$, respectively. Let us consider the path explored for inputs $k \in [0, 127]$. While exploring the path, we record a sequence of symbolic memory addresses

$\langle \&p[k], \&q[255 - k], \&p[k] \rangle$, where $\&x$ denotes the address of value x . Since we started execution with an empty cache, the first access to $p[k]$ inevitably incurs a cache miss, irrespective of the value of k . The subsequent accesses can either be cold misses (first access to the respective cache line) or eviction misses (non-first access to the respective cache line). Let us consider the second access to $p[k]$, as this is the memory access that partitions the input space. In order to check whether the second access to $p[k]$ is a cold miss, we check the following constraint:

$$(0 \leq k \leq 127) \wedge (set(\&p[k]) \neq set(\&q[255 - k])) \wedge (set(\&p[k]) \neq set(\&p[k])) \quad (1)$$

where $set(\&x)$ captures the cache line where memory address $\&x$ is mapped to. Intuitively, the constraint checks whether access to $p[k]$ touches a cache line for the first time. Constraint (1) is clearly *unsatisfiable*, leading to the fact that the second access to $p[k]$ does not access a cache line for the first time during execution.

Subsequently, we check whether the second access to $p[k]$ can suffer an eviction miss. To this end, we check whether $q[255 - k]$ can evict $p[k]$ from the cache as follows:

$$(0 \leq k \leq 127) \wedge (set(\&p[k]) = set(\&q[255 - k])) \wedge (tag(\&p[k]) \neq tag(\&q[255 - k])) \quad (2)$$

where $tag(\&x)$ captures the cache tag associated with the accessed memory block. Intuitively, Constraint (2) is satisfied if and only if $q[255 - k]$ accesses a different memory block as compared to $p[k]$, but $q[255 - k]$ and $p[k]$ access the same cache line (hence, causing an eviction before $p[k]$ was accessed for the second time). In this way, we collect Constraints (1)-(2) to formulate the cache behaviour of a memory access into $\Gamma(0 \leq k \leq 127)$.

After constructing $\Gamma(0 \leq k \leq 127)$, we explore the path for inputs $k \in [128, 255]$ and record the sequence of memory accesses $p[k]$, $q[k - 128]$ and $p[k]$. Performing a similar exercise, we can show that the second access to $p[k]$ cannot be a cold miss along this path. In order to check whether the second access to $p[k]$ was an eviction miss along this path, we check whether $q[k - 128]$ can evict $p[k]$ from the cache as follows:

$$(128 \leq k \leq 255) \wedge (set(\&p[k]) = set(\&q[k - 128])) \wedge (tag(\&p[k]) \neq tag(\&q[k - 128])) \quad (3)$$

Constraint (3) is used to formulate $\Gamma(128 \leq k \leq 255)$ and is unsatisfiable. This is because only $p[0]$ shares a cache line with $q[255]$ (i.e. $set(\&p[0]) = set(\&q[255])$) and therefore, $set(\&p[k]) = set(\&q[k - 128])$ is evaluated *false* for $128 \leq k \leq 255$. As a result, the second access to $p[k]$ is not a cache miss for any input $k \in [128, 255]$.

From the observation $\langle m, m, m \rangle$, we know that the second access to $p[k]$ was a miss. From the discussion in the preceding paragraph, we also know that this observation cannot occur for any inputs $k \in [128, 255]$. Therefore, the value of k must result in Constraint (2) satisfiable. Constraint (2) is unsatisfiable if we restrict the value of k between 1 and 127. This happens based on the fact that

only $p[0]$ is mapped to the same cache line as $q[255]$ (cf. Figure 2(d)). As a result, CHALICE reports 255 (127 for the `if` branch and 128 for the `else` branch in Figure 2(a)) values being leaked for the observation $\langle m, m, m \rangle$. In other words, CHALICE accurately reports the information leak (i.e. $k = 0$) for the observation $\langle m, m, m \rangle$.

3. Framework

In the following, we formally introduce the problem statement and provide an outline of our overall approach to solve this problem.

3.1. Foundation

Threat model. Side-channel attacks are broadly classified into synchronous and asynchronous attacks [25]. In synchronous attack, an attacker can trigger the processing of known inputs (e.g. a plain-text or a cipher-text for encryption routines), whereas such a phenomenon is not possible for asynchronous attacks. Synchronous attacks are clearly easier to perform, since the attacker does not need to compute the start and end of the targeted routine under attack. For instance, in synchronous attack, the attacker can trigger encryption of known plaintext messages and observe the encryption-timing [11]. Since CHALICE is a software validation tool with the aim of producing side-channel resistant implementations, we assume the presence of a strong attacker in this paper. Therefore, we consider the attacker can request and observe the execution (e.g. number of cache miss) of the targeted routine. We also assume that the attacker can execute arbitrary user-level code in the same processor running the targeted routine. This allows the attacker to flush the cache before the targeted routine starts execution and therefore, reduce the external noise in the observation. The attacker, however, is incapable to access the address space of the target routine.

Notations. The execution of program \mathcal{P} on input I results in an execution trace t_I . t_I is a sequence over the alphabet $\Sigma = \{h, m\}$ where h (respectively, m) represents a cache hit (respectively, cache miss). Our proposed method in CHALICE quantifies the information leaked through t_I . We capture this quantification via $\mathcal{L}(t_I)$. We assess the information leakage with respect to an *observer*. An *observer* is a mapping $\mathcal{O} : \Sigma^* \rightarrow \mathbb{D}$ where \mathbb{D} is a countable set. For instance, an observer $\mathcal{O} : \Sigma^* \rightarrow \mathbb{N}$ can count the number of misses and will associate both sequences $\langle m, h, m, h, h \rangle$ and $\langle m, m, h, h, h \rangle$ to 2. It will therefore not differentiate them. The most precise observer would be the identity mapping on Σ^* . However, an observer that tracks prefixes of some fixed lengths (for example 2) would be enough to differentiate the two aforementioned sequences.

We use the variable $miss_i$ to capture whether or not the i -th memory access was a cache miss during execution. The observation by an attacker, over the execution for an arbitrary input and according to the observer model \mathcal{O} , is considered via the observation constraint $\Phi_{\mathcal{O}}$.

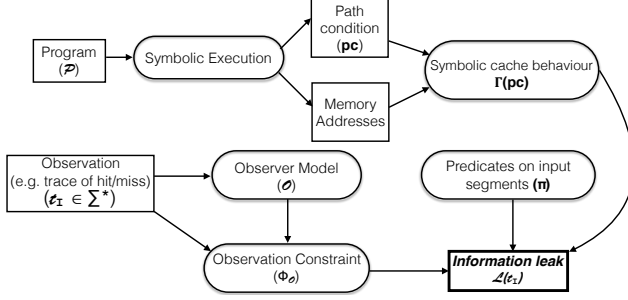


Figure 3. The framework CHALICE.

Φ_O is a symbolic constraint over the set of variables $\{miss_1, miss_2, \dots, miss_n\}$, where n is the total number of memory accesses during an execution. For instance, $\Phi_O \equiv (\sum_{i=1}^n miss_i = 100)$ accurately captures that the attacker observes 100 cache misses in an execution manifesting n memory accesses. For the sake of formulation, we use $\Phi_{O,e}$ to define a *projection* of Φ_O on an arbitrary program path e . In particular, $\Phi_{O,e}$ captures the observation constraint if program path e is executed. Given only Φ_O to be observed by an attacker, CHALICE quantifies how much information about the respective program input is leaked.

The central idea of our information leak detection is to capture the cache behaviour via symbolic constraints. Let us consider a set of inputs \mathbb{I} that exercise the same execution path with n memory accesses. We use $\Gamma(\mathbb{I})$ to accurately encode all possible combinations of values of variables $\{miss_1, miss_2, \dots, miss_n\}$. Therefore, if $\Gamma(\mathbb{I}) \wedge \Phi_O$ is *unsatisfiable*, we can deduce that the respective observation Φ_O *did not occur* for any input $I \in \mathbb{I}$.

We now describe how $\mathcal{L}(t_I)$ is computed based on the notations and the intuition mentioned in the preceding.

3.2. Quantifying Information Leak in Execution

Figure 3.1 provides an outline of our entire framework. We symbolically execute a program \mathcal{P} compute the path condition [18] for each explored path. Such a path condition symbolically encodes all program inputs for which the respective program path was followed. Our symbolic execution based framework tracks all memory accesses on a taken path and therefore, enables us to characterize, for all symbolic arguments satisfying the path condition, the set of all associated cache behaviors.

Recall that we use $\Gamma(\mathbb{I})$ to capture possible cache hit/miss sequences in an execution path, which was activated by a set of inputs \mathbb{I} . In an abuse of notation, we capture set of inputs \mathbb{I} via path conditions. For instance, in Figure 2(a), we use $\Gamma(0 \leq k \leq 127)$ to encode all possible cache hit/miss sequences for inputs activating the `if` branch.

For an arbitrary execution path, let us consider pc be the path condition. Along this path, we record each memory access and we consider its cache behaviour via variable $miss_i$. $miss_i$ is set to 1 (resp. 0) if and only if the i -th memory access along the path encounters a cache miss (hit). Given n to be the total number of memory accesses

along the path, we formulate $\Gamma(pc)$ to bound the value of $\{miss_1, miss_2, \dots, miss_n\}$. In particular, any solution of $\Gamma(pc) \wedge (miss_i = 1)$ captures a concrete input $I \Rightarrow pc$ and such an input I leads to an execution where the i -th memory access is a cache miss. Therefore, if an observation Φ_O happens to be for input $I \Rightarrow pc$, $\Gamma(pc) \wedge \Phi_O$ is always satisfiable.

We capture the information leak through execution trace t_I as follows:

$$\mathcal{L}(t_I) = 2^N - \left| \bigvee_{e \in Path} (\Gamma(pc_e) \wedge \Phi_{O,e}) \right|_{sol} \quad (4)$$

where N is size of program input (in bits), $\Phi_{O,e}$ is the projection of the observation constraint on path e , $Path$ is the set of all program paths and pc_e is the path condition for program path e . $|\mathcal{X}|_{sol}$ captures the number of solutions satisfied by predicate \mathcal{X} . It is worthwhile to note that $|\bigvee_{e \in Path} (\Gamma(pc_e) \wedge \Phi_{O,e})|_{sol}$ accurately captures the number of program inputs that exhibit the observation satisfied by Φ_O . In other words, Equation (4) quantifies the number of program inputs that does not exhibit the observation, as captured by Φ_O . Hence, if the attacker observes Φ_O , she can deduce as many as $\mathcal{L}(t_I)$ inputs were impossible for the respective observation.

In practice, however, computing the exact value of $\mathcal{L}(t_I)$ might be infeasible, as it might require the enumeration of all solutions. In order to control such enumeration, we generate predicates on input variables. In particular, we sample an N -bit input into K equal segments, resulting in input segments of length $\frac{N}{K}$. Subsequently, we constrain the search space of the solver by restricting the value of each such input segment to any possible value, that is, pointing to a value in the set $\{0, 1, \dots, 2^{\frac{N}{K}} - 1\}$. For instance, let us assume x is the program input and x_i captures the i -th input segment. A predicate $\pi \equiv (x_i = 0)$ will guide the solver to search for a solution only in the input space where the i -th input segment is 0. Since, we have K different segments, we generate a total of $(K \cdot 2^{\frac{N}{K}})$ different predicates. For each such predicate π , we record information leak if the following constraint is *unsatisfiable*:

$$\bigvee_{e \in Path} (\Gamma(pc_e) \wedge \Phi_{O,e} \wedge \pi) \quad (5)$$

Concretely, if Constraint (5) is unsatisfiable, we can accurately record that input I , which leads to observation Φ_O along some program path, satisfies the predicate $\neg\pi$. An appealing feature of this process is that all $K \cdot 2^{\frac{N}{K}}$ predicates can be generated independently and therefore, the unsatisfiability check of Constraint (5) can be performed in parallel for different predicates.

Let us assume, $\mathcal{U}_1, \mathcal{U}_2, \dots, \mathcal{U}_K$ are the number of unsatisfiable solutions reported for each of the K input segments respectively. Therefore, we can estimate a lower bound on $\mathcal{L}(t_I)$ from these unsatisfiability checks as follows:

$$\mathcal{L}(t_I) \geq 2^N - \prod_{1 \leq i \leq K} \left(2^{\frac{N}{K}} - \mathcal{U}_i \right) \quad (6)$$

Due to the classic path explosion problem in symbolic execution, it is possible that only a subset of paths $\mathcal{P}' \subseteq \text{Path}$ can be explored within a given time budget. In such cases, we can quantify $\mathcal{L}(t_I)$ as follows.

$$\begin{aligned}
\mathcal{L}(t_I) &= 2^N - \left| \bigvee_{e \in \text{Path}} (\Gamma(pc_e) \wedge \Phi_{\mathcal{O},e}) \right|_{\text{sol}} \\
&= \left| \bigvee_{e \in \mathcal{P}'} pc_e \right|_{\text{sol}} + \left| \bigvee_{e \in \text{Path} \setminus \mathcal{P}'} pc_e \right|_{\text{sol}} \\
&- \left| \bigvee_{e \in \mathcal{P}'} (\Gamma(pc_e) \wedge \Phi_{\mathcal{O},e}) \right|_{\text{sol}} \\
&- \left| \bigvee_{e \in \text{Path} \setminus \mathcal{P}'} (\Gamma(pc_e) \wedge \Phi_{\mathcal{O},e}) \right|_{\text{sol}} \quad (7) \\
&\geq \left| \bigvee_{e \in \mathcal{P}'} pc_e \right|_{\text{sol}} - \left| \bigvee_{e \in \mathcal{P}'} (\Gamma(pc_e) \wedge \Phi_{\mathcal{O},e}) \right|_{\text{sol}} \\
&\geq \left| \bigvee_{e \in \mathcal{P}'} pc_e \right|_{\text{sol}} - \prod_{1 \leq i \leq K} \left(2^{\frac{N}{K}} - \mathcal{U}_i \right)
\end{aligned}$$

This result follows from the fact that $\Gamma(pc_e) \wedge \Phi_{\mathcal{O},e} \Rightarrow \Gamma(pc_e) \Rightarrow pc_e$. The term $\left| \bigvee_{e \in \mathcal{P}'} pc_e \right|_{\text{sol}}$ involves only path conditions and it can be computed via model counting [5].

Finally, it is worthwhile to note that setting $K = 1$ is equivalent to enumerating all solutions as in Equation (4). In contrast, setting $K = N$ is equivalent to checking information leak at bit-level (*i.e.* checking whether the value of a single bit can influence cache performance). Therefore, K provides a tunable parameter for different levels of information leak detection. We have conducted evaluation for $K = 8$ and $K = N$. This means, we have checked how much information about a single byte and respectively, a single bit are leaked through observing cache performance.

In the next section, we will describe the construction of $\Gamma(pc)$ for an arbitrary path condition pc .

4. Generating Symbolic Cache Model

The technical contribution of our methodology is a symbolic model for cache behaviour – establishing a link between the program input and observed cache performance. To describe our model, we shall use the following notations throughout our discussions:

- $2^{\mathcal{S}}$: The number of cache sets in the cache.
- $2^{\mathcal{B}}$: The size of a cache line (in bytes).
- \mathcal{A} : Associativity of cache. For direct-mapped caches, $\mathcal{A} = 1$.
- $\text{set}(r_i)$: Cache set accessed by instruction r_i .
- $\text{tag}(r_i)$: The tag stored in the cache for the memory block accessed by r_i .
- ζ_i : The cache state before executing instruction r_i and after executing instruction r_{i-1} .

In the following, we will explain the different steps of generating the symbolic cache model.

4.1. Intercepting Memory Requests

We symbolically execute a program P . During symbolic execution, we track the path condition and the sequence of memory accesses for each explored path. For instance, while symbolically exercising the `if` branch of Figure 2(a), we track the path condition $0 \leq k \leq 127$ and the sequence of memory addresses $\langle \&p[k], \&q[255 - k], \&p[k] \rangle$. It is worthwhile to note that such memory addresses might capture symbolic expressions due to the dependency from program inputs. Concretely, we compute the path condition pc and the execution trace Ψ_{pc} for each explored path as follows:

$$\Psi_{pc} \equiv \langle (r_1, \sigma_1), (r_2, \sigma_2), \dots, (r_{n-1}, \sigma_{n-1}), (r_n, \sigma_n) \rangle \quad (8)$$

where r_i captures the i -th memory-related instruction executed along the path and σ_i symbolically captures the memory address accessed by r_i .

4.2. Modeling Symbolic Cache Access

In order to find the impact on caches, we need to find out the set of cache lines being accessed. This is accomplished by manipulating the expression σ_i , which was collected while executing each memory-related instruction r_i (*cf.* Equation (8)). In particular, we formulate $\text{set}(r_i)$ as follows:

$$\text{set}(r_i) = (\sigma_i \gg \mathcal{B}) \ \& \ (2^{\mathcal{S}} - 1) \quad (9)$$

In Equation (9), “ $\&$ ” captures a bitwise-and operation and “ \gg ” captures a right-shift operation.

Apart from the cache set a memory address is mapped to, we need to distinguish different memory addresses from which contents are stored into the cache. This is different from just checking the inequality between σ_i values, as the memory controller groups contents of different memory addresses into a *memory block* and stores the memory block into a cache line. In order to distinguish different memory blocks mapped into the same cache lines, a tag is stored within each cache line. For instruction r_i , such a tag $\text{tag}(r_i)$ is captured as follows:

$$\text{tag}(r_i) = (\sigma_i \gg (\mathcal{B} + \mathcal{S})) \quad (10)$$

Therefore, if $\text{tag}(r_i) \neq \text{tag}(r_j)$, we can conclude that r_i and r_j are accessing different memory blocks, even if $\text{set}(r_i) = \text{set}(r_j)$ holds.

It is worthwhile to note that both $\text{set}(r_i)$ and $\text{tag}(r_i)$ might be symbolic expressions due to the presence of symbolic expression σ_i in Equations (9)-(10). Moreover, the computations of $\text{set}(r_i)$ and $\text{tag}(r_i)$ are independent of any cache replacement policy.

4.3. Direct-mapped Caches

In this section, we assume that the cache is *direct-mapped*. Therefore, each cache set holds exactly one cache line. In the next section, we extend our symbolic model for set-associative caches.

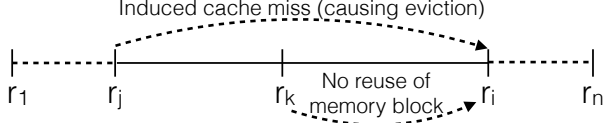


Figure 4. Memory-access r_j induces a cache miss at r_i if r_j accesses the same cache set as r_i and r_k does not load the block accessed by r_i

We characterize cache misses into the following two categories:

- 1) Cold cache misses. r_i suffers a cold miss *if and only if* $set(r_i)$ has not been accessed by any previous instruction $r \in \{r_1, r_2, \dots, r_{i-1}\}$.
- 2) Cache misses due to eviction. r_i suffers a cache miss due to eviction *if and only if* the last access to $set(r_i)$ had been from an instruction $r_j \in \{r_1, r_2, \dots, r_{i-1}\}$, such that $tag(r_j) \neq tag(r_i)$.

Constraints to formulate cold cache misses. If a cache line is accessed for the *first time*, such an access will inevitably incur a cache miss. Let us consider that we want to check whether instruction r_i accesses a cache line for the first time during execution. In other words, we can check none of the instruction $r \in \{r_1, r_2, \dots, r_{i-1}\}$ touches the same cache line as r_i . Therefore r_i suffers a cold miss if and only if the following condition holds:

$$\Theta_i^{cold} \equiv \bigwedge_{p \in [1, i)} (set(r_p) \neq set(r_i)) \quad (11)$$

Constraints to formulate cache evictions. In the following, we formulate a set of constraints to encode cache misses other than cold cache misses. Such cache misses occur due to the eviction of memory blocks from caches.

To illustrate different cache-miss scenarios clearly, let us consider the example shown in Figure 4. Assume that we want to check whether r_i will suffer a cache miss due to eviction. This might happen only due to instructions appearing before (in the program order) r_i . Consider one such instruction r_j , for some $j \in [1, i)$. Informally, r_j is responsible for a cache miss at r_i , *only if* the following conditions hold:

- 1) $\psi_{cnf}(j, i)$: r_i and r_j access the same cache set. Therefore, we have the following constraint:

$$\psi_{cnf}(j, i) \equiv (set(r_j) = set(r_i)) \quad (12)$$

- 2) $\psi_{dif}(j, i)$: r_i and r_j access different memory-block tags. This can be formalized as follows:

$$\psi_{dif}(j, i) \equiv (tag(r_j) \neq tag(r_i)) \quad (13)$$

- 3) $\psi_{eqv}(j, i)$: There does not exist any instruction r_k where $k \in [j+1, i)$, such that r_k accesses the same memory block as r_i . It is worthwhile to note that the existence of r_k will load the memory block accessed at r_i . Since r_k is executed after r_j (in program order), r_j must not be responsible for

a cache miss at r_i . We formulate the following constraint to capture this condition:

$$\psi_{eqv}(j, i) \equiv \bigwedge_{k: j < k < i} (tag(r_k) \neq tag(r_i) \vee set(r_k) \neq set(r_i)) \quad (14)$$

Constraints (12)-(14) capture necessary and sufficient conditions for instruction r_j to replace the memory block accessed by r_i (where $j < i$) and the respective block not being accessed between r_j and r_i . In order to check whether r_i suffers a cache miss due to eviction, we need to check Constraints (12)-(14) for any $r \in \{r_1, r_2, \dots, r_{i-1}\}$. This can be captured via the following constraint:

$$\Theta_i^{emp} \equiv \left(\bigvee_{j: 1 \leq j < i} (\psi_{cnf}(j, i) \wedge \psi_{dif}(j, i) \wedge \psi_{eqv}(j, i)) \right) \quad (15)$$

r_i will not suffer a cache miss due to eviction when at least one of the Constraints (12)-(14) does not hold for all prior instructions of r_i . This scenario is the negation of Constraint (15) and therefore, it is captured via $\neg \Theta_i^{emp}$.

We use variable $miss_i$ to capture whether instruction r_i suffers a cache miss. As discussed in the preceding paragraphs, r_i suffers a cold miss (*i.e.* satisfying Constraint (11)) or the memory block accessed by r_i would be evicted due to instructions executed before r_i (*i.e.* satisfying Constraint (15)). Using this notion, we formulate the value of $miss_i$ as follows:

$$\Theta_i^{mp, dir} \equiv (\Theta_i^{emp} \vee \Theta_i^{cold}) \quad (16)$$

$$\Theta_i^{m, dir} \equiv (\Theta_i^{mp, dir} \Rightarrow (miss_i = 1)) \quad (17)$$

$$\Theta_i^{h, dir} \equiv (\neg \Theta_i^{mp, dir} \Rightarrow (miss_i = 0)) \quad (18)$$

Putting it all together. Recall that $\Gamma(pc)$ captures the constraint system to encode the cache behaviour for all inputs $I \Rightarrow pc$. In order to construct $\Gamma(pc)$, we gather constraints, as derived in the preceding sections, and the path condition into $\Gamma(pc)$ as follows:

$$\Gamma(pc) \equiv pc \wedge \bigwedge_{i \in [1, n]} (\Theta_i^{m, dir} \wedge \Theta_i^{h, dir}) \quad (19)$$

4.4. Set-associative Caches

In direct-mapped caches, exactly one memory-block tag is contained by a cache set. As a result, this memory block is replaced by any instruction accessing the same cache set, but accessing a different memory-block tag. In contrast, set-associative caches group multiple cache lines into a cache set. Therefore, evicting a memory block from a cache set might require multiple accesses to the respective cache set. The number of such accesses, as required to evict a memory block from a cache set, is determined by the relative position of the same block within the cache set. This relative position is updated during execution according to a cache

replacement policy. In this paper, we instantiate CHALICE for set-associative caches with LRU replacement policy.

From technical perspective, we need to modify Constraints (15)-(18) to reflect the working principle of set-associative caches. Before discussing such modifications, we introduce the concept of *cache conflict*, which is crucial for formulating the cache behaviour of set-associative caches.

Definition 4.1. (Cache Conflict): r_j generates a cache conflict to r_i only if executing r_j can influence the relative position of memory block accessed by r_i within the cache state ζ_i (i.e. the cache state before r_i and after r_{i-1}).

In order to check whether r_i suffers a cache miss, we distinguish between the following two scenarios:

- 1) r_i accesses a memory block for the first time. Hence, r_i will suffer a cold cache miss.
- 2) The number of unique cache conflicts generated to r_i is sufficient to evict the memory block accessed by r_i . Hence r_i will suffer a cache miss.

Constraints to formulate cold cache misses. If r_i accesses a memory block for the first time, the following condition must hold:

$$\Theta_i^{cold} \equiv \bigwedge_{1 \leq k < i} (tag(r_k) \neq tag(r_i) \vee set(r_k) \neq set(r_i)) \quad (20)$$

Informally, Constraint (20) states that every instruction $r \in \{r_1, r_2, \dots, r_{i-1}\}$ either accesses a different cache set than $set(r_i)$ or the accessed memory block has a different tag compared to $tag(r_i)$. This leads to a cold cache miss at r_i .

Constraints to formulate cache evictions. The eviction of a memory block from the cache is critically influenced by cache conflict. Therefore, we need to consider all scenarios where a cache conflict might be generated. For LRU caches, r_j generates a cache conflict to r_i (where $j < i$) only if the following conditions hold:

- 1) $\psi_{cnf}(j, i)$, $\psi_{dif}(j, i)$ and $\psi_{eqv}(j, i)$ hold (cf. Constraints (12)-(14)). This ensures that r_j and r_i access the same cache set, but different memory-block tags. Additionally, $\psi_{eqv}(j, i)$ ensures that there does not exist any instruction between r_j and r_i that loads the memory block accessed by r_i .
- 2) Note that multiple accesses may influence the cache content in set-associative caches. Therefore, we need to distinguish unique memory accesses in order to formulate cache conflict. For instance, consider the following memory accesses in sequence: $r_1:m_1 \rightarrow r_2:m_2 \rightarrow r_3:m_2 \rightarrow r_4:m_1$, where r_i captures the instruction and m_j captures the respective memory block being accessed. If m_1 and m_2 map to the same cache set in a 2-way LRU cache, r_4 will still be a cache hit. This is because r_4 suffers cache conflict only once, from the access to memory block m_2 , even though m_2 has been accessed twice (at r_2 and at r_3). In order to account

unique cache conflicts, we only record the cache conflict from the *closest* access to different memory blocks. For instance, in the preceding example, we only record cache conflict from r_3 to r_4 . Formally, we need additional constraints to distinguish such closest accesses. We use the constraint $\psi_{unq}(j, i)$ for such purpose. $\psi_{unq}(j, i)$ is satisfiable if and only if there does not exist any instruction between r_j (where $j \in [1, i)$) and r_i that accesses the same memory block as r_j . $\psi_{unq}(j, i)$ is formalized as follows:

$$\psi_{unq}(j, i) \equiv \bigwedge_{k: j < k < i} (tag(r_j) \neq tag(r_k) \vee set(r_j) \neq set(r_k)) \quad (21)$$

Constraints (12)-(14) and Constraint (21) accurately capture scenarios where r_j ($j \in [1, i)$) will create a unique cache conflict to r_i . Let us assume $\Psi_{i,j}^{evt}$ captures whether r_j creates a unique cache conflict to r_i . Using the intuition described in the preceding paragraph, we can formulate the following constraints to set the value of $\Psi_{i,j}^{evt}$.

$$\Theta_{j,i}^{em} \equiv (\psi_{cnf}(j, i) \wedge \psi_{dif}(j, i) \wedge \psi_{eqv}(j, i) \wedge \psi_{unq}(j, i)) \Rightarrow (\Psi_{j,i}^{evt} = 1) \quad (22)$$

If any of the conditions in Constraints (12)-(14) and in Constraint (21) is not satisfied between r_j and r_i , then we do not account for the cache conflict between r_j and r_i , as captured by the following formulation:

$$\Theta_{j,i}^{eh} \equiv (\neg\psi_{cnf}(j, i) \vee \neg\psi_{dif}(j, i) \vee \neg\psi_{eqv}(j, i) \vee \neg\psi_{unq}(j, i)) \Rightarrow (\Psi_{j,i}^{evt} = 0) \quad (23)$$

We use variable $miss_i$ to capture whether r_i is a cache miss. Therefore, $miss_i$ is set to 1 if r_i is a cache miss, and is set to 0 otherwise. We formulate the value of $miss_i$ using the following constraints:

$$\Theta_i^{mp, lru} \equiv \left(\sum_{j \in [1, i)} \Psi_{j,i}^{evt} \geq \mathcal{A} \right) \vee \Theta_i^{cold} \quad (24)$$

$$\Theta_i^{m, lru} \equiv \left(\Theta_i^{mp, lru} \Rightarrow (miss_i = 1) \right) \quad (25)$$

$$\Theta_i^{h, lru} \equiv \left(\neg\Theta_i^{mp, lru} \Rightarrow (miss_i = 0) \right) \quad (26)$$

In Constraint (24), \mathcal{A} captures the associativity of the cache. Once a memory block is loaded into the cache, it requires at least \mathcal{A} unique cache conflicts to evict the block. If $\Psi_{i,j}^{evt} \geq \mathcal{A}$, r_i has suffered at least \mathcal{A} unique cache conflicts since the last access of the memory block referenced by r_i – resulting r_i to be a cache miss. If r_i is not a cold miss (i.e. $\neg\Theta_i^{cold}$ holds) and it has not suffered \mathcal{A} unique cache conflicts, r_i will be a cache hit, as captured by Constraint (26).

Putting it all together. To derive the symbolic cache behavior $\Gamma(pc)$, we gather all constraints over $\{r_1, \dots, r_n\}$ and the path condition pc as follows:

$$\Gamma(pc) \equiv pc \wedge \bigwedge_{i \in [1, n]} \left(\Theta_i^{m, lru} \wedge \Theta_i^{h, lru} \wedge \bigwedge_{j \in [1, i]} \Theta_{j, i}^{em} \wedge \bigwedge_{j \in [1, i]} \Theta_{j, i}^{eh} \right) \quad (27)$$

$\Theta_i^{m, lru}$ and $\Theta_i^{h, lru}$ together bound the value of $miss_i$, which, in turn captures whether r_i is a cache miss. However, $\Theta_i^{m, lru}$ and $\Theta_i^{h, lru}$ are dependent on symbolic variables $\Psi_{j, i}^{evt}$ where $j \in [1, i]$. The bound on $\Psi_{j, i}^{evt}$ is captured via $\Theta_{j, i}^{em}$ and $\Theta_{j, i}^{eh}$ (Constraints (22)-(23)). Hence, the formulation of $\Gamma(pc)$ includes both $\Theta_{j, i}^{em}$ and $\Theta_{j, i}^{eh}$ for $j \in [1, i]$.

Complexity of constraints. The size of our constraint system, in order to check cache side-channel leaks, is $O(n^3)$. Here n is the number of memory accesses. The dominating factor in our constraint system is the set of constraints generated from Constraint (15) and Constraint (22). In general, we generate constraints for each pair of memory accesses that may potentially conflict in the cache, leading to $O(n^2)$ pairs in total. For each such pair, the constraint may have a size $O(n)$ — making the size of overall constraint system to be $O(n^3)$. However, our evaluation reveals that such a bound is pessimistic and the constraint system can be solved efficiently for real-life embedded programs.

5. Checking Information Leak

In this section, we instantiate CHALICE for two different observer models. In particular, we show the formulation of Equation (5) by leveraging on our symbolic cache model $\Gamma(pc)$ (as described in Sections 4.3-4.4) and instantiating Φ_O for different observer models. We assume that t_I is the observed execution trace for input I and we wish to quantify how much information about input I is leaked through t_I .

Observation via total miss count. In this scenario, an attacker can observe the number of cache misses in different executions [11]. The observer $\mathcal{O} : \Sigma^* \rightarrow \mathbb{N}$ is a function, where a sequence of cache hits and misses are mapped to a non-negative integer capturing the number of cache misses. Therefore, for a given trace $t \in \Sigma^*$, $\mathcal{O}(t)$ captures the number of cache misses in the trace t .

Recall that we use variable $miss_i$ to capture whether the i -th memory access was a cache miss. We check the unsatisfiability of the following logical formula to record information leak:

$$\bigvee_{e \in Path} \left(\Gamma(pc_e) \wedge \left(\sum_{i \in [1, n_e]} miss_i = \mathcal{O}(t_I) \right) \wedge \pi \right) \quad (28)$$

where n_e is the number of memory accesses occurring along path e and π is a predicate defined on program inputs. Concretely, if Constraint (28) is unsatisfiable, we can establish that the information “ $\neg\pi \equiv true$ ” is leaked through

the execution trace t_I . By performing such unsatisfiability checks over the entire program input space, we quantify the information leak $\mathcal{L}(t_I)$ through execution trace t_I (cf. Equation (6)).

Observation via hit/miss sequence. For an execution trace $t \in \Sigma^*$, an observer can monitor hit/miss sequences from t [6]. Concretely, let us assume $\{o_1, o_2, \dots, o_k\}$ is the set of positions in trace t where the observation occurs. If n is the total number of memory accesses in t , we have $o_i \in [1, n]$ for each $i \in [1, k]$.

We define the observer $\mathcal{O} : \Sigma^* \rightarrow \{0, 1\}^k$ as a projection from the execution trace onto a bitvector of size k . Such a projection satisfies the following conditions: $\mathcal{O}(t)_i = 1$ if $t_{o_i} = m$ and $\mathcal{O}(t)_i = 0$ otherwise. $\mathcal{O}(t)_i$ captures the i -th bit of $\mathcal{O}(t)$ and similarly, t_{o_i} captures the o_i -th element in the execution trace t . Note that a strong observer could map the entire execution trace to a bitvector of size n .

For such an observer, we check the unsatisfiability of the following formula to record information leak:

$$\bigvee_{e \in Path} \left(\Gamma(pc_e) \wedge \bigwedge_{i \in \{1, 2, \dots, k\}} \left(\bigwedge_{o_i \leq n_e} miss_{o_i} = \mathcal{O}(t_I)_i \right) \wedge \pi \right) \quad (29)$$

where π is a predicate on program inputs. By generating such predicates over the input space, we quantify the information leaked about input I via $\mathcal{L}(t_I)$ (cf. Equation (6)).

Although we instantiate CHALICE for two observer models, we believe that our framework is generic to capture a wide range of such models. In particular, we can tune CHALICE for any observer model that is expressed via symbolic constraints over variables $miss_i$.

6. Implementation Aspects

In this section, we discuss some crucial implementation aspects for the efficiency and effectiveness of CHALICE.

Implementation setup. We implemented CHALICE on top of the KLEE symbolic virtual machine [2]. However, in order to design such an implementation, we faced the following challenges.

```

/* load local variable */
load reg1, 16[@Sp]
beq reg1, 127, L2
L1: load reg2, 24[@Sp]
    br L3
L2: load reg2, 32[@Sp]
L3: add reg1, reg2
/* register spill */
store reg1, 16[@Sp]
load reg1, 40[@Sp]
sub reg1, reg2

/* load local variable */
%0 = getelementptr i8*, @Sp, i8 16
%1 = load i8*, %0
%2 = icmp eq i8 %1, 127
br i1 %2, label L1, label L2
L1: %3 = getelementptr i8*, @Sp, i8 24
    %4 = load i8*, %3
    br label L3
L2: %5 = getelementptr i8*, @Sp, i8 32
    %6 = load i8*, %5
L3: %7 = phi i8 [%4, L1], [%6, L2]
    %8 = add i8 %1, %7
/* register spill */
store i8 %1, i8* %0
%9 = getelementptr i8*, @Sp, i8 40
%10 = load i8*, %9
%11 = sub i8 %10, %7

```

(a) Binary code, assume all loads are loading bytes

(b) Translated LLVM code, some details are removed for clarity

Figure 5. Translation from binary code to LLVM code

KLEE works on LLVM bytecode [4]. Considering cache performance, at the level of LLVM bytecode, introduces several inaccuracies. For instance, LLVM bytecode uses an unbounded number of virtual registers. In contrast, any given execution platform only contains a finite number of physical registers. In order to understand how this impacts memory performance, consider the example in Figure 5.

In Figure 5, we assume that the execution platform contains only two physical registers. As a result, a register spill is required in the binary code to preserve the functionality of the LLVM bytecode. In general, aggressive compiler optimizations may change the structure and memory behaviour of the LLVM bytecode dramatically, when translated into native binary.

In order to solve this challenge and still use the power of symbolic execution on target-independent LLVM bytecode, we have designed a translator that converts binary code to LLVM bytecode. Such a translation must preserve the following properties to produce a valid LLVM bytecode. First, we ensure that each load/store instruction in the binary code to have a functionally equivalent load/store instruction in the translated bytecode. Secondly, we preserve the static-single-assignment (SSA) form of LLVM bytecode by systematically inserting *Phi* functions. Thirdly, several instructions at the machine code may require multiple LLVM instructions to implement. The `LWL` and `LWR` are such machine-level instructions for MIPS architecture. Finally, LLVM bytecode is strongly typed. As a result, LLVM bytecode uses different instructions for pointer arithmetic as compared to general-purpose arithmetic. We use a lightweight type inference on the binary code and compute the appropriate LLVM instruction for a given machine-level instruction. Figure 5(b) demonstrates how the example binary code is translated into LLVM bytecode. The instruction `getelempttr` handles pointer arithmetic in the LLVM bytecode.

From a technical point of view, we have designed a translator that converts PISA binaries (a MIPS like architecture) into LLVM bytecode. Such a translator is unique in the sense that it focuses on preserving the memory behaviour during the translation. Nevertheless, our translator may introduce additional instructions to preserve the SSA semantics of LLVM bytecode. Such additional instructions are not part of the binary code. In order to exclude such instructions from our analysis, we annotate the LLVM bytecode with a mapping from each memory-related instruction in the binary to the respective memory-related instruction in the LLVM bytecode. As a result, CHALICE accurately captures the cache side-channel leaks for applications compiled into PISA binaries.

Our translator currently does not handle indirect jump instructions. However, we can use a lightweight static analysis to compute the potential targets for indirect jumps and the translator can easily be modified to take this into account. Besides, CHALICE is modular in the sense that it can easily be adapted for a different architecture. This can be accomplished only by extending the translator to convert the respective machine code into LLVM bytecode.

Program	Lines of C code	Lines of LLVM code	Max. #Memory access
AES [1]	800	4950	2134
AES [3]	1428	1800	420
DES [3]	552	3990	334
RC4 [3]	160	668	1538
RC5 [3]	256	1820	410
gdk_keyval_to_unicode	1300	268	114
gdk_keyval_name	1350	1408	12

TABLE 1. SALIENT FEATURES OF THE EVALUATED SUBJECT PROGRAMS

Reducing the number of constraints. In order to reduce the size of $\Gamma(pc)$, we first inspect constraints generated for each memory-related instruction individually. In particular, for each memory-related instruction r_i , we check whether the respective memory access leads to a cache miss (or hit) for all inputs satisfying pc . For instance, consider Constraints (17)-(18) for direct-mapped caches. In order to check whether instruction r_i is a miss for all inputs $I \Rightarrow pc$, we check the validity of the constraint $pc \wedge \Theta_i^{mp,dir}$. Similarly, we check the unsatisfiability of the constraint $pc \wedge \Theta_i^{mp,dir}$, to prove that r_i is always a cache hit for all inputs $I \Rightarrow pc$. If $pc \wedge \Theta_i^{mp,dir}$ is valid (resp. unsatisfiable), we can directly consider $miss_i$ to be 1 (resp. 0) within the symbolic cache model $\Gamma(pc)$. As a result, we discard all constraints $\Theta_i^{m,dir}$ and $\Theta_i^{h,dir}$ in formulating $\Gamma(pc)$. It is worthwhile to note that this optimization increases the time to process a single memory-related instruction, as the solver is called at each memory access. However, we discovered that in practice, this step dramatically reduces the size of $\Gamma(pc)$, making our information leak detection tractable.

7. Evaluation

Experimental setup. In order to evaluate the effectiveness of CHALICE, we have chosen cryptographic applications from OpenSSL library [3] and other software repository [1], as well as applications from Linux GDK library. The choice of our subject programs is motivated by the critical importance of validating security-related properties in these applications. Some salient features of the evaluated subject programs is outlined in Table 1. We have performed all our experiments on an Intel I7 machine with 8GB of RAM and running Debian as operating systems.

7.1. Generating Predicates on Inputs

Using CHALICE, we can select an arbitrary number of bits in the program input to be symbolic. These symbolic bits capture the high sensitivity of the input subspace and our framework focuses to quantify the information leaked about this subspace. For instance, in encryption routines, the bits of private input (e.g. a secret key) can be made symbolic. Without loss of generality, in the following discussion, we assume that the entire input is sensitive and we make all input bits to be symbolic.

Let us assume N -byte program input. We use the notation $k[i]$ to capture the i -th byte of an arbitrary input k . Similarly, we use $k[i, j]$ to capture the j -th bit of the i -th

byte in k . We generate the following predicates on inputs for quantifying information leak $\mathcal{L}(t_I)$ (cf. Equation (6)).

$$\mathbf{P}_{\text{bit}} = \{k[i, j] = v \mid i \in [1, N], j \in [1, 8], v \in [0, 1]\}$$

$$\mathbf{P}_{\text{byte}} = \{k[z] = v \mid i \in [1, N], v \in [0, 255]\}$$

It is worthwhile to mention that for a 16-byte sensitive input (e.g. in AES-128), \mathbf{P}_{bit} and \mathbf{P}_{byte} lead to 256 and 4096 calls to the solver, respectively to quantify $\mathcal{L}(t_I)$.

7.2. Experience with AES-128

We used two different implementations [1], [3] of the Advanced Encryption Standard (AES). AES is a widely used encryption standard for achieving confidential communication. AES has been of great importance for delivering security in embedded systems because of its sound protection strength and high throughput (e.g. even on credit cards). Therefore, it is crucial to validate security-related properties, such as side-channel resistance, for AES.

AES has input-dependent memory accesses. In particular, different encryption rounds of AES revolve around accessing an `sbox` – a matrix-like structure kept in main memory (DRAM). During encryption, AES code accesses varied locations in the `sbox`. The location of the `sbox` being accessed, for a given instruction, depends on the secret key. That is, the sequence of memory blocks, accessed during encryption, is dependent on the value of secret key. As a result, we potentially obtain different cache performance for different secret keys.

7.2.1. Key result. We used an 8 KB direct-mapped cache with a line size of 32 bytes. This size is big enough to keep the entire `sbox` of AES in the cache. We executed AES in simplescalar simulator [8] (cf. Figure 1) with a test suite and obtained the respective set of observations (e.g. number of cache misses). For such observations, we intended to check how much information is leaked through a bit or a byte, by generating predicates P_{bit} and P_{byte} (as described in Section 7.1), respectively.

For the collected set of observations, CHALICE quantifies $\mathcal{L}(t_I)$ to be 0 when the set of predicates P_{bit} is used. Therefore, each observation (e.g. the number of cache misses) is possible irrespective of whether an arbitrary bit of the AES input (in both implementations of AES [1], [3]) is “1” or “0”. Therefore we deduce, for the given set of observations, *there does not exist any dependency between the cache performance and the value of an arbitrary bit of the key.*

Figure 6(a) captures an outline of information leak highlighted via CHALICE, for two different implementations of AES [1], [3]. For each byte of the 16-byte secret key, we show the amount of information leaked through the number of cache misses. For instance, we establish for certain observations, that as many as 251 values (out of 256) are leaked for each byte of AES key (in the implementation [1]). *This means, there exists at least 251^{16} possible keys (out of a total 2^{128}) that can be eliminated just by observing*

the cache misses. Such an information gives the designer valuable insights when designing embedded systems, both in terms of choosing an AES key and a cache architecture, in order to avoid serious security breaches. In contrast to the implementation of [1], we can observe from Figure 6(a) that the implementation of AES from OpenSSL exhibits substantially fewer information leaks. For instance, certain key bytes of OpenSSL AES do not leak any information through the number of cache misses.

In our framework, we also investigated on adversaries who can observe the sequence of cache hits and misses, instead of just the overall number of cache misses. However, to simplify our evaluation, we focused on sequences of length 1, and considered all the memory accesses. Our goal is to check the dependency between the AES-key and the hit/miss characteristics of an arbitrary memory access.

Figure 6(b) captures a snapshot of dependencies between AES-key bytes and the cache behavior of different memory accesses. For instance, the maximum values leaked through a byte can be as high as 235, as shown via Figure 6(b). Similar to Figure 6(a), we also observe that the AES implementation from OpenSSL leaks substantially less information, as compared to the implementation in [1], when cache behavior is observed individually for each memory access.

7.2.2. Sensitivity of Information Leak w.r.t Cache Size.

Figures 7-8 capture the sensitivity of information leakage with respect to different configurations. For all experiments, the replacement policy is set to LRU and the cache-line size is set to a fixed 32 bytes. Figures 7(a)-(b) captures the information-leakage-sensitivity for observations via a given number of cache misses. Increasing cache size (or associativity) may have two contrasting effects as follows. For a given cache size, let us assume a subset of the input space $\mathbb{I}_{=C} \subseteq \mathbb{I}_{<C} \cup \mathbb{I}_{=C} \cup \mathbb{I}_{>C}$ (where $\mathbb{I}_{<C} \cup \mathbb{I}_{=C} \cup \mathbb{I}_{>C}$ is the entire input space) which leads to C cache misses. Increasing cache size reduces cache conflict. Therefore, it is possible that some input $i \in \mathbb{I}_{>C}$, which leads to more than C cache misses with a smaller cache, produces C cache misses with the increased cache size. This tends to increase the number of inputs leading to C cache misses, thus reducing the amount of information leaked through observing C misses. Secondly, some input $i \in \mathbb{I}_{=C}$ may have less than C cache misses with increased cache size. This may reduce the number of inputs having C cache misses, thus increasing the potential leakage through the observation of C cache misses. In Figure 7(a), the reduction in cache side-channel leakage is visible for cache sizes up to 16 KB, for AES implementation from [1]. However, for a 4-way 32 KB cache, we observe the increase in information leakage. This is because the number of possible keys, leading to a given observation, is reduced considerably.

Figures 8(a)-(b) capture the sensitivity of information leakage (w.r.t. cache size) for an adversary who can observe the cache behavior of an arbitrary memory access. Concretely, consider the bars in Figure 8(a) for 8 KB and 32 KB caches. For a 2-way, 8 KB cache, a significant information about the first key byte is leaked. With 32 KB

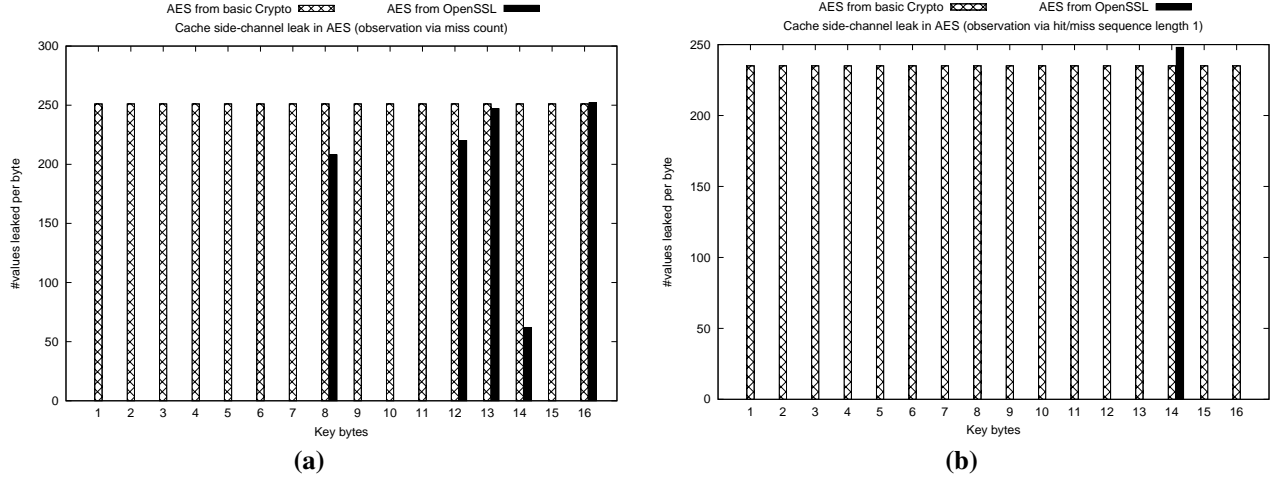


Figure 6. Information leak observed using an 8 KB direct-mapped cache

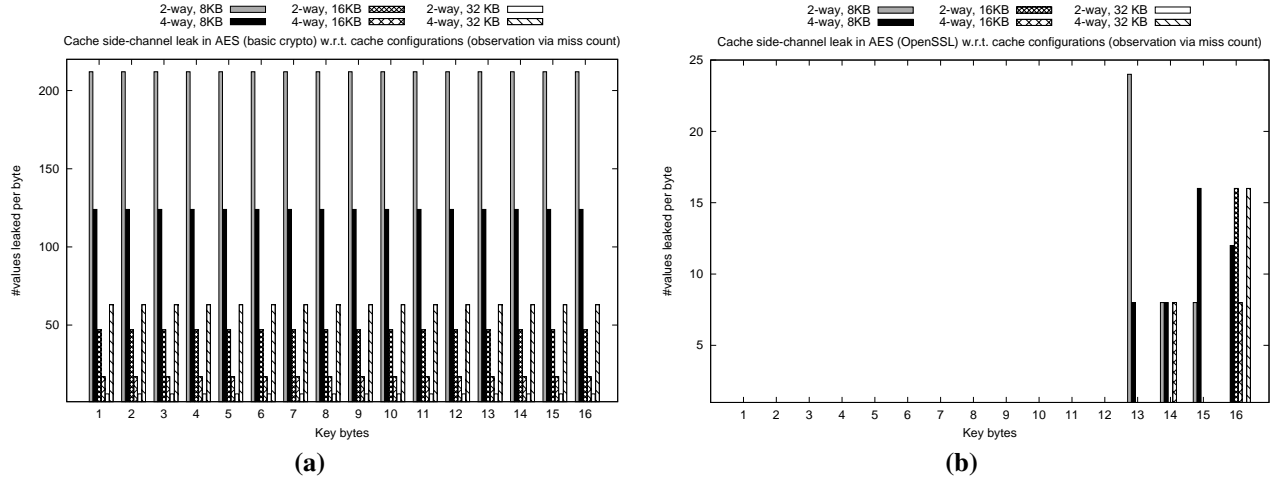


Figure 7. Information leak in AES w.r.t. observations based on miss count (set-associative caches employing LRU policy)

caches, the number of cache conflicts reduces substantially, but we observe substantial leakage of information about key bytes one, six and ten. Therefore, even though the increased cache size improves performance, it might make the overall system potentially less secure, as shown in Figure 8(b). In summary, we believe such insights are valuable for designers to build secure systems.

The evaluation also reveals that the AES implementation from OpenSSL exhibits information leak, as shown in Figure 8(b). Figure 8(b) highlights the last four bytes of the key to experience more leakage of information as compared to other key bytes.

7.3. Experience with DES

Data Encryption standard (DES) [3] is a symmetric key algorithm for electronic data. The OpenSSL implementation of DES encrypts 64 bit message with a 64 bit secret key. Figures 9(a)-(b) summarize our result on quantifying information leak in DES. Figure 9(a) reports information leaks through observing miss count. For instance, using

8KB caches, DES leaks more than 150 values for several key bytes. In contrast, information leak in the OpenSSL version of AES is relatively sparse and it generally leaks less information about key bytes (*cf.* Figure 7(b)). In Figure 9(b), we observe a similar trend, as DES continues to suffer from information leak when the cache behavior of an arbitrary memory access is observed. Our results summarize potentially insecure nature of DES, even if we only consider security leaks through cache behaviour.

7.4. Experience with RC4

RC4 [3] is a stream cipher. It uses variable length key (between 40 and 2048 bits) and it is considered to be vulnerable in many applications. In our evaluation, we studied how RC4 leaks information through cache side channels. We analyzed the OpenSSL version of RC4 implementation, where we fixed the size of key to be 64 bits. Figures 10(a)-(b) outline our findings. Figure 10(a) summarizes our results for miss-count-based observer models. CHALICE highlights information being leaked about the first byte. For bigger

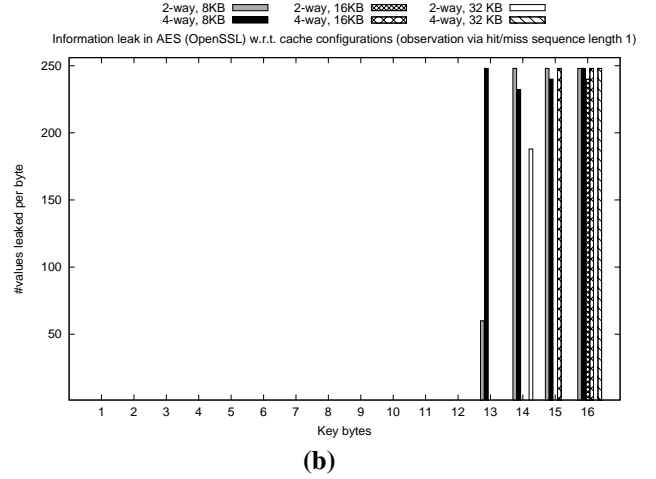
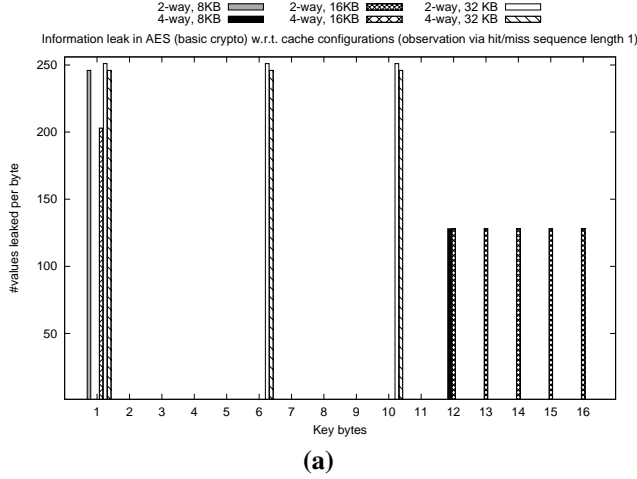


Figure 8. Information leak in AES w.r.t. observations based on hit/miss sequence

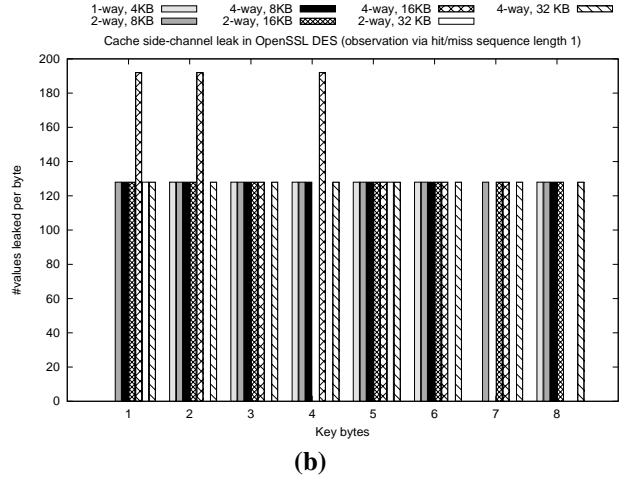
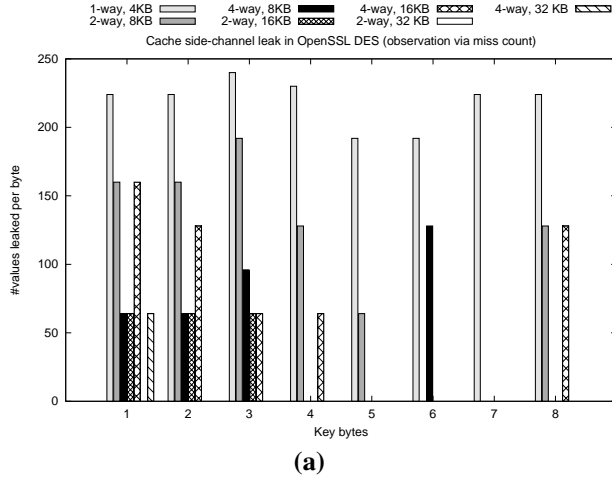


Figure 9. Information leak in DES w.r.t. different observer models

cache sizes (*e.g.* > 16KB), such information leak disappears, as the executions of RC4 only suffer the minimum number of misses to load all the memory blocks into the cache.

Figure 10(b) highlights information leaks when the cache hit/miss characteristics of arbitrary memory accesses are observed. With respect to such observations, we identify that a substantial information may leak (254 values out of a total of 256) about the first byte. However, with bigger cache sizes, such information leak disappears.

7.5. Experience with RC5

RC5 [3] is a symmetric block cipher, which is suitable for both software and hardware implementation. RC5 has a variable word size and a variable-length secret key. In our evaluation, we analyzed the RC5 implementation available in the OpenSSL library and we fixed size of both the plaintext and the secret key to be 16 bytes.

During the execution of RC5, our tool CHALICE does not report any symbolic memory address. This means, for any memory-related instruction, the referenced address is

independent of secret key. As a result, cache performance (*i.e.* number of cache misses or the sequence of hits and misses) of RC5 is unrelated to input and does not exhibit information leak with respect to the observer models studied in this paper. It is also worthwhile to mention that RC5 does not have any key-dependent branches. Therefore, we can turn the report generated by CHALICE into verification, meaning that we can prove the absence of information leak according to the observer models explored in this paper.

7.6. Experience with GDK Library

Figures 11(a)-(b) present the average information leak discovered in routines `gdk_keyval_to_unicode` and `gdk_keyval_name` from the Linux GDK library. As shown in Figure 11, several scenarios lead to a complete disclosure of information for the third and the fourth byte of input (*i.e.* 255 out of 256 values are leaked for these bytes). Moreover, the reported information leak persists across a wide-range of cache configurations. Upon close inspection, we discovered that the cache behaviour of

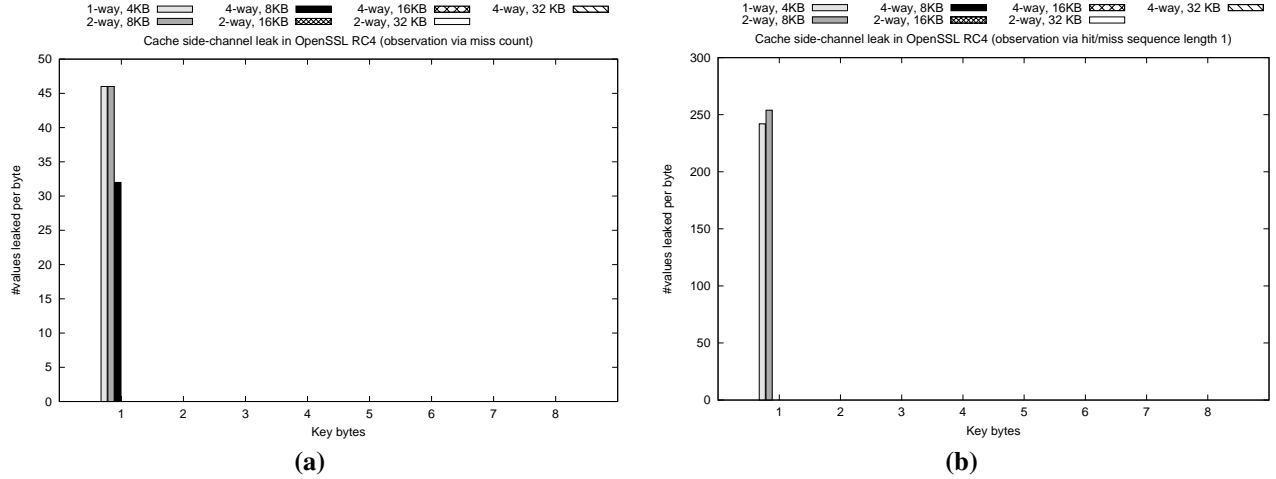


Figure 10. Information leak in RC4 w.r.t. different observer models

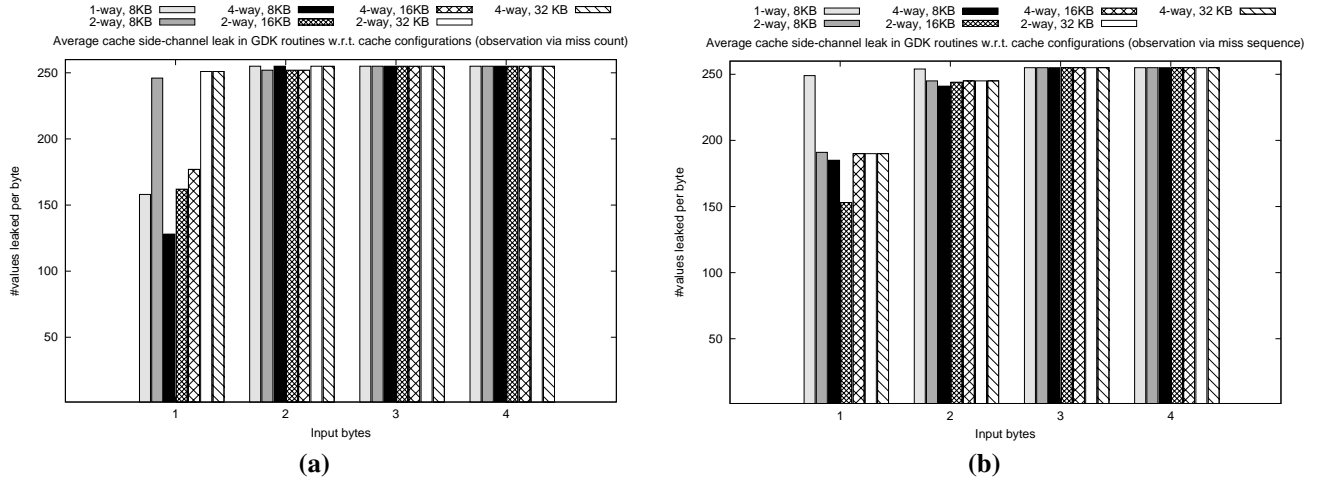


Figure 11. Information leak in Linux GDK library w.r.t. different observer models

TABLE 2. T_1 CAPTURES AVERAGE TIME TAKEN FOR ONE SOLVER CALL, T_{byte} CAPTURES THE AVERAGE TIME TAKEN TO CHECK INFORMATION LEAK FOR ONE INPUT BYTE AND T_{all} CAPTURES THE TIME TAKEN TO CHECK INFORMATION LEAK VIA ALL PREDICATES IN \mathbf{P}_{byte} (cf. SECTION 7.1)

Subject program	Observation via total miss count					Observation via hit/miss of an arbitrary access				
	Constraint size	Peak mem.	T_1	T_{byte}	T_{all}	Constraint size	Peak mem.	T_1	T_{byte}	T_{all}
AES [1]	144072	261M	≈ 20 sec	1 hour	16 hours	1580	105M	< 1 sec	≈ 1 min	16 min
AES [3]	21444	129M	≈ 18 sec	77 min	20 hours	265	90M	< 1 sec	≈ 2 min	45 min
DES [3]	53808	127M	≈ 10 sec	50 min	8 hours	1809	35M	< 1 sec	≈ 1 min	12 min
RC4 [3]	38622	1.1G	≈ 4 sec	15 min	4 hours	490	32M	< 1 sec	≈ 1 min	16 min
RC5 [3]	0	28.3M	≈ 15 sec	≈ 15 sec	≈ 15 sec	0	29.2M	≈ 14 sec	≈ 14 sec	≈ 14 sec
GDK	21	102M	< 1 sec	< 1 sec	≈ 2 min	21	100M	< 1 sec	< 1 sec	≈ 1 min

`gdk_keyval_to_unicode` and `gdk_keyval_name` is primarily dominated by the number of cold cache misses, which, in turn is heavily influenced by the path executed in the respective routine. As a result, observing the cache performance may lead to a disclosure of the (set of) paths taken in `gdk_keyval_to_unicode` and `gdk_keyval_name`. Since we include path condition pc within our symbolic cache model $\Gamma(pc)$ (cf. Constraint (19) and Constraint (27)), we can accurately quantify the information leak even in the presence of multiple program paths.

7.7. Analysis Time

Table 2 outlines the analysis time for different subject programs while using a direct-mapped 8KB cache. In most cases, a single call to the solver, which reports information leak via unsatisfiability check (e.g. Constraint (5)), is efficient. Due to the repeated calls to solver, checking the information leakage, for the entire input space, takes significant time. However, CHALICE incorporates *anytime* strategy, meaning the more time it runs the more accurately it can quantify the information leak. Besides, the timing reported in Table 2 is either consistent or decreases with

increasing cache size. This is due to the fact that our symbolic cache model uses the notion of cache conflict to encode the cache behaviour and the size of our model does not vary dramatically with increasing cache size. Finally, the performance of CHALICE can be improved drastically using a parallel implementation. For instance, we can assign one or more independent threads to check information leaked about each input byte. We plan to implement such a parallel version of CHALICE in the future. Table 2 only reports timing for a sequential implementation in this paper.

7.8. Discussion

For the sake of brevity, we have only presented the quantification of information leak discovered through CHALICE. Of course, due to the symbolic nature of our analysis, CHALICE not only quantifies information leak, it also highlights which values might leak through a potential cache attack. Furthermore, for each memory-related instruction, CHALICE highlights the set of input values that may leak for a given execution. In summary, the report generated by CHALICE can be leveraged for debugging and fixing critical information leak scenarios. Some of the potential debugging strategies would be to restructure the code, suppressing or enabling compiler optimizations (such as bypassing the cache for certain memory blocks or using software-controlled memory) and choosing an appropriate hardware platform. In future, we plan to use CHALICE to study the impact of such hardware/software transformations on information leak.

8. Related Work

The closest to our work are approaches based on static analysis [16], [21]. These works quantify information leak from the static representation of a program. In particular, the information leak is quantified via the unique number of observations made by an attacker. As a result, these works are incapable to highlight critical information leak scenarios when a particular observation leaks substantially more information than the rest. CHALICE quantifies information leak from execution traces and therefore, it does not suffer from the aforementioned limitation. Our work is orthogonal to approaches proposed in [7], [10]. In particular, our approach targets arbitrary software binaries and it is not limited to the verification of constant-time cryptographic software. Besides, our approach has a significant flavor of testing and debugging, as we highlight information leak scenarios directly from execution traces. A recent work [22] aims to quantify side-channel leakage via symbolic execution and Max-SMT. However, this work does not take into account side-channel leaks through micro-architectural entities, such as caches.

Over the last few decades, cache-based side-channel attacks have emerged to be a prevalent class of security breaches for many systems. A detailed account on these attacks can be found in the survey [17]. The observer models used in this paper are based on existing cache attacks [6],

[11]. However, we believe that CHALICE is generic to incorporate more advanced attack scenarios [12], [19], [20], as long as the attacks are expressed via the intuition given in Section 5.

To defend against cache-based side-channel attacks, several countermeasures have been proposed over the past few years. Some of these countermeasures require hardware support, such as designing new cache architecture [26] or compiler support, such as devising new instruction-based scheduling [23]. More recently, the approach described in [14] leverages on software diversity at runtime to randomize the cache behavior and hence, reducing the probability for a potential cache side-channel attack. Our proposal is orthogonal to approaches proposing countermeasures. Of course, we believe that our framework can be leveraged as a valuable tool to discover potential flaws in countermeasures proposed to mitigate cache side channels.

Finally, static cache analysis [24] is still an active research topic. Compared to static cache analysis, our approach has significant flavors of testing and debugging. Moreover, our approach can highlight memory accesses that leak significant information via side-channels. This can be leveraged to drive security-related optimizations.

In summary, we propose a new approach to quantify cache side-channel leakage from execution traces and *not* from the static representation of the program. We demonstrate that such an approach clearly has benefits over approaches based on static or logical analysis. This is because CHALICE can highlight critical information leak scenarios that are impossible to be discovered by competitive static or logical analysis.

9. Concluding Remarks

In this paper, we propose a new approach to quantify cache side-channel leakage. To the best of our knowledge, CHALICE is the first work to categorize input segments with respect to memory performance. We illustrate that the mechanism of CHALICE is highly desirable for security testing of arbitrary software, specifically, to detect the amount of information that can leak through memory performance. Besides security testing, CHALICE can also be used to discover bugs while writing constant-time cryptographic applications. We demonstrate the usage of CHALICE to highlight critical information leak scenarios in real-world software – including applications from OpenSSL and Linux GDK libraries.

We believe CHALICE provides a platform to lift the state-of-the-art in security testing, in particular, detecting security-related flaws due to side channels. As a result, we envision to extend CHALICE for side channels other than caches and use it to detect the potential of advanced side-channel attacks not investigated in this paper. We hope that the core idea of CHALICE would influence regular activities in software testing and in testing regressions.

References

- [1] Advanced Encryption Standard Implementation. <https://github.com/B-Con/crypto-algorithms>.
- [2] KLEE LLVM execution engine. <https://klee.github.io/>.
- [3] OpenSSL Library. <https://github.com/openssl/openssl/tree/master/crypto>.
- [4] The LLVM compiler infrastructure. <http://llvm.org/>.
- [5] UC Davis, Mathematics. Latte integrale. <https://www.math.ucdavis.edu/~latte/>.
- [6] Onur Açıgmez and Çetin Kaya Koç. Trace-driven cache attacks on AES. In *Information and Communications Security*. Springer, 2006.
- [7] José Bacelar Almeida, Manuel Barbosa, Gilles Barthe, François Dupressoir, and Michael Emmi. Verifying constant-time implementations. In *USENIX*, pages 53–70, 2016.
- [8] Todd Austin, Eric Larson, and Dan Ernst. SimpleScalar: An infrastructure for computer system modeling. *Computer*, 35(2), 2002.
- [9] Earl T Barr, Mark Harman, Phil McMinn, Muzammil Shahbaz, and Shin Yoo. The oracle problem in software testing: A survey. *IEEE transactions on software engineering*, 41(5):507–525, 2015.
- [10] Gilles Barthe, Gustavo Betarte, Juan Diego Campo, Carlos Daniel Luna, and David Pichardie. System-level non-interference for constant-time cryptography. In *CCS*, pages 1267–1279, 2014.
- [11] Daniel J Bernstein. Cache-timing attacks on AES, 2005.
- [12] Billy Bob Brumley and Risto M Hakala. Cache-timing template attacks. In *ASIACRYPT*. Springer, 2009.
- [13] James Clause, Wanchun Li, and Alessandro Orso. Dytan: a generic dynamic taint analysis framework. In *ISSTA*. ACM, 2007.
- [14] Stephen Crane, Andrei Homescu, Stefan Brunthaler, Per Larsen, and Michael Franz. Thwarting cache side-channel attacks through dynamic software diversity. In *NDSS*, 2015.
- [15] John Demme, Robert Martin, Adam Waksman, and Simha Sethumadhavan. Side-channel vulnerability factor: A metric for measuring information leakage. In *ISCA*, 2012.
- [16] Goran Doychev, Boris Köpf, Laurent Mauborgne, and Jan Reineke. CacheAudit: a tool for the static analysis of cache side channels. *TISSEC*, 18(1):4, 2015.
- [17] Qian Ge, Yuval Yarom, David Cock, and Gernot Heiser. A survey of microarchitectural timing attacks and countermeasures on contemporary hardware. In *Cryptology ePrint Archive*, 2016. <https://eprint.iacr.org/2016/613.pdf/>.
- [18] Patrice Godefroid, Nils Klarlund, and Koushik Sen. DART: directed automated random testing. In *PLDI*, 2005.
- [19] Daniel Gruss, Raphael Spreitzer, and Stefan Mangard. Cache template attacks: Automating attacks on inclusive last-level caches. In *USENIX Security*, 2015.
- [20] David Gullasch, Endre Bangerter, and Stephan Krenn. Cache games—bringing access-based cache attacks on AES to practice. In *IEEE Symposium on Security and Privacy*. IEEE, 2011.
- [21] Boris Köpf, Laurent Mauborgne, and Martín Ochoa. Automatic quantification of cache side-channels. In *CAV*. Springer, 2012.
- [22] Corina S. Pasareanu, Quoc-Sang Phan, and Pasquale Malacaria. Multi-run side-channel analysis using symbolic execution and max-smt. In *CSF*, 2016.
- [23] Deian Stefan, Pablo Buiras, Edward Z Yang, Amit Levy, David Terei, Alejandro Russo, and David Mazières. Eliminating cache-based timing attacks with instruction-based scheduling. In *ESORICS*, pages 718–735. Springer, 2013.
- [24] Henrik Theiling, Christian Ferdinand, and Reinhard Wilhelm. Fast and precise WCET prediction by separated cache and path analyses. *Real-Time Systems*, 18(2-3), 2000.
- [25] Eran Tromer, Dag Arne Osvik, and Adi Shamir. Efficient cache attacks on aes, and countermeasures. *Journal of Cryptology*, 23(1):37–71, 2010.
- [26] Zhenghong Wang and Ruby B. Lee. New cache designs for thwarting software cache-based side channel attacks. In *ISCA*, pages 494–505, 2007.